Available online at www.sciencedirect.com
ScienceDirect
C. R. Mecanique 337 (2009) 481–491
COMPTES RENDUS MECANIQUE

Combustion for aerospace propulsion

Liquid sheet disintegration at high pressure: An experimental approach

V.G. Fernandez *, P. Berthoumie, G. Lavergne

ONERA (Office national d'études et de la recherche aérospatiales), Heterogeneous, Multiphase Flows Unit, Aerodynamic and Energetic Models Department, BP 4025, 2, avenue Edouard-Belin, 31055 Toulouse cedex 4, France

Available online 29 July 2009

Abstract

The primary atomization was studied in a 300 μm thickness water sheet, generated by a planar airblast atomizer. The research novelty consisted in increasing the airflow absolute pressure from atmospheric conditions to 6 bar. The experimental techniques employed included Oscillometry by Laser Intensity Reflexion (ORIL), Laser Doppler Velocimetry (LDV) and flow visualization by fast video camera. The atomization mechanisms, described in the literature at atmospheric environments, were observed at high pressure conditions, for a constant momentum flux ratio. Furthermore, a new atomization mechanism was observed at high values of this ratio. Finally, dimensionless relations have been proposed for the global oscillation frequency, minimum air oscillation velocity, break-up distance and transversal wavelength. ***To cite this article: V.G. Fernandez et al., C. R. Mecanique 337 (2009).***

Résumé

Atomisation d'une nappe liquide à haute pression : approche expérimentale. L'atomisation primaire a été étudiée sur une nappe d'eau de 300 μm d'épaisseur, générée par un injecteur de type aérodynamique. L'objectif de cette recherche a consisté à étudier l'influence de la pression environnante sur les mécanismes d'atomisation dans une plage de 1 à 6 bar. Les techniques expérimentales retenues ont concerne l'Oscillométrie par la Réflexion de l'Intensité Laser (ORIL), la vélocimétrie laser (LDV) et la visualisation par camera vidéo rapide. Les mécanismes d'atomisation, décrits dans la littérature, à la pression atmosphérique, ont été observés en conditions de pression élevées, pour un même rapport de flux de quantité de mouvement entre les deux fluides. Un nouveau mécanisme d'atomisation a été mis en évidence à haute pression. Des corrélations reliant des nombres adimensionnels sont proposées pour quantifier la fréquence d'oscillation globale, la vitesse minimale d'oscillation d'air, la longueur de rupture et la longueur d'onde de l'instabilité transversale de la nappe liquide. ***Pour citer cet article : V.G. Fernandez et al., C. R. Mecanique 337 (2009).***

Keywords: Fluid mechanics; Primary break-up; High pressure testing; Airblast atomizer

Mots-clés : Mécanique des fluides ; Atomization primaire ; Essais haute pression ; Atomiseur aérodynamique

* Corresponding author.
E-mail address: Vital.Gutierrez_Fernandez@onera.fr (V.G. Fernandez).

1631-0721/$ – see front matter
doi:10.1016/j.crme.2009.06.026

Nomenclature

c_{inj}	Airblast cord length ..... m	μ	Dynamic viscosity ..... kg/ms
f_{Gl}	Global oscillation frequency ..... Hz	ρ	Density ..... kg/m^3
L_b	Break-up length ..... m	σ	Surface tension ..... N/m
t_g	Air characteristic length: air duct side length ..... m		
t_l	Liquid characteristic length: liquid sheet thickness ..... m		
v	Fluid velocity ..... m/s		
V_{min}	Minimum air oscillation velocity ..... m/s		

Dimensionless numbers

$M = \rho_g v_g^2 / \rho_l v_l^2$ Momentum flux ratio
$Re = \rho v t / \mu$ Reynolds number
$We = \rho_l v^2 t / \sigma$ Weber number
$Str = f_{Gl} t_l / V_{min}$ Strouhal number

Greek letters

δ	Boundary layer thickness ..... m	l	Liquid
δ_ω	Vorticity thickness ..... m	g	Air
$\lambda_\perp$	Transversal wavelength ..... m	δ	Boundary layer thickness

Subscripts

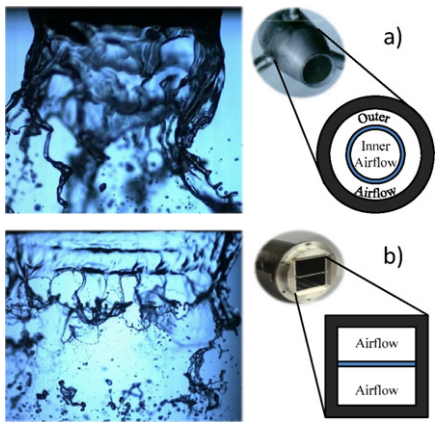

Fig. 1. Liquid disintegration in a) an annular sheet, b) a planar sheet.

1. Introduction

Ever since the experiments accomplished by Savart [1] in 1833, liquid sheets have been readily used to study liquid atomization processes. Indeed, at the ONERA (French Aerospace Laboratory), this geometry has been repeatedly chosen, in experimental [2] and numerical [3] approaches, to analyze the primary atomization. In the current research, its new high pressure facility LACOM (Multiphase COmbustion LAboratory) has been employed to investigate this phenomenon. The objective was to determine the pressure influence on the primary atomization behaviour.

Airblast atomizers are commonly trusted to disintegrate the kerosene in turbine engines. This is due to their greater efficiency, at generating small size droplets, in continuous-flow systems, with relative low airflow velocities [4]. Briefly, the airblast atomizer injects a liquid sheet between two parallel airflows. The longitudinal and transversal instabilities, which eventually atomize the liquid film, are a consequence of the interaction between these fluid flows. In Fig. 1, it may be compared to the liquid sheets generated by an annular and a planar simplified geometries of these devices.

In the fuel injection domain, there is an important distinction between liquid fragmentation from a continuous flow into droplets and that from a given droplet, into smaller ones. The former case is called primary atomization, while the latter is referred to as secondary atomization. In this research, we focused on the first, which took place close to the injector's edge, less than 5 mm for most flow configurations.

Real turbine airblast atomizers have always favoured an annular geometry. Nevertheless, in this investigation a planar geometry was chosen. This was due to its simpler design, more accessible to optical techniques. Furthermore, it has been established that their dynamic behaviours may be compared, as long as, the annular airblast atomizer has a diameter greater than 1 cm, [5,6]. This was the case of our research, Fig. 1b.

2. Experimental set-up and procedure

One of the causes behind the complexity in the primary atomization experimental tests and computational models, has been the great quantity of factors affecting its behaviour. The most fundamental research has compared the effect of varying the fluids' velocities or different inner–outer gas velocities [7]. Once this has been done, researchers have focused in studying the effect of the liquid sheet thickness and/or the airflow outlet cross sectional area [8]. Assuredly, tests have been accomplished with various fuels or liquids [9], or with a given liquid, whose surface tension and dynamic viscosity was modified [10].

It is worth mentioning an exhaustive investigation performed by Mansour and Chigier [11], who compared the sheet oscillating behaviour with a hard spring system. In this characterization, the liquid sheet global oscillation frequency, at different fluids velocities, could be use to distinguish three dynamic behaviour modes. Following their example, as well as, the one of Larricq [2], we intended to remain within their flow configurations, as the absolute pressure increased.

2.1. Flow conditions

The first parameter adjusted was the airflow velocity. It went from 20 m/s to 70 m/s. The gas absolute pressure increased from an atmospheric environment up to 6 bars. This corresponded to a modest value compared to the 10 bars in helicopter or the 40 bars in aeroplane turbine engines. Nevertheless, it provided a valuable insight into the liquid sheet primary atomization behaviour. It should be mention that to keep the air velocity constant, the air mass flow was increased accordingly with each higher pressure. The liquid injected was water at 1 and 2 m/s.

Considering the fluid flows previously described, the experimental activity was characterised by the following dimensionless parameters: The gas Reynolds number, with the atomizer chord as characteristic length, ranged from a transitional value of 1.2×10^5 to a turbulent magnitude of 2.5×10^6. The water Reynolds number, with the liquid sheet thickness as characteristic length, went from 150 to 600. The Weber number, We, had a valued as low as 1.8 and up to 142, its characteristic length was again the injector's chord. The momentum flux ratio, M, increased from 0.5 to 35.5.

Finally, a set of measurements was carried out at atmospheric conditions, with a liquid injection velocity equal to 0.5 m/s. This was done to compare the primary atomization at ambient conditions with that at high pressure for a constant momentum flux ratio.

2.2. Experimental set-up

The sketch in Fig. 2 shows the injection line, in the LACOM facility. It might be observed how, after the pipe's elbow, an annular-hole screen was installed. Its purpose was to guarantee an uniform airflow velocity profile, at the airblast atomizer. In addition to that, a square duct (46×46 mm) was placed after the elbow, with a length greater than 30 times its equivalent diameter. Following the airflow, at the end of this duct, an averaging Pitot tube was positioned to measure the flow velocity before the airblast atomizer. In the Fig. 2 zoom, our atomizer is shown. It had a NACA 63-010 profile, with a 89 mm chord length and it generated a thin liquid sheet, 300 μm thickness and 40 mm width. Ultimately, the injector's lips had a thickness of 700 μm. Immediately after the injector, within the visualization chamber, a second duct with the same square section, was fitted. This duct avoided the undesired recirculation effect, on the liquid sheet. Finally, the airflow velocity in the vessel was modified with the digital valve installed at the end of the injection line. The experimental techniques operated were:

– *High Speed Camera Visualization*: A Phantomv.9 model was used. As with any fast camera, there was a compromise between image size and acquisition rate. Consequently, it was decided to take two sets of visualizations at each flow condition. The first one with images 580×864 pixels (11.56×17.2 mm) recorded at 3000 Hz, to

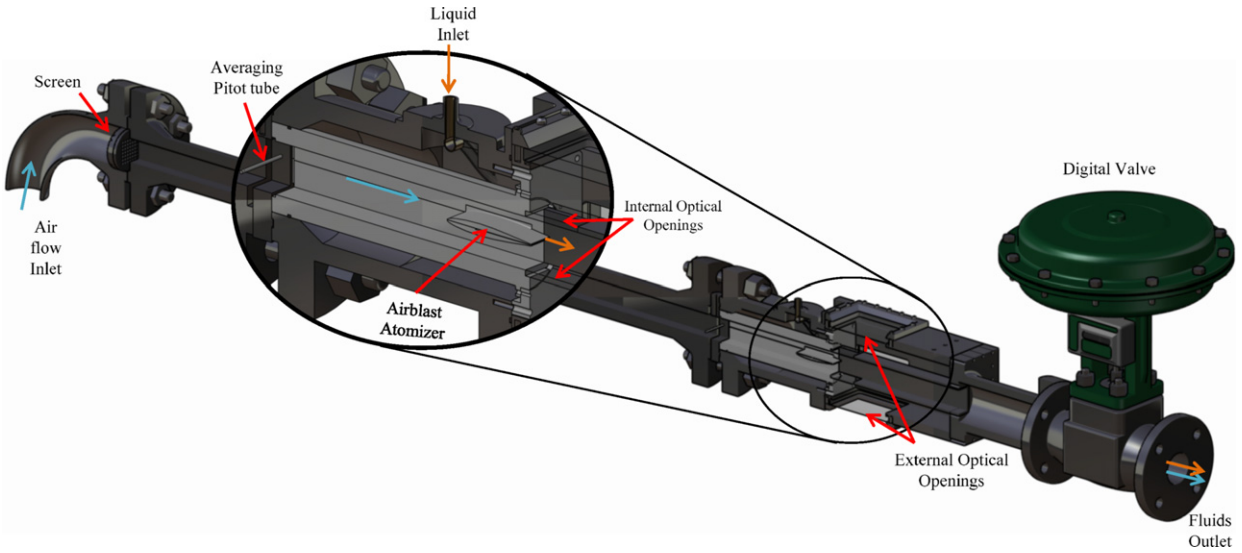

Fig. 2. Injection line. Detail: Zoom on the airblast atomizer.

measure space dependable variables, such as, the break-up length or separation between ligaments. The second one, with images 368 × 720 pixels (7.57 × 14.4 mm) size recorded at 6000 Hz, to measure time dependent variables, like ligament diameter and length. In order to obtain the magnitude of these variables, a semi-automatic post imaging process was required.

– *OLIR (Oscillometry by Laser Intensity Reflexion) technique*: a Laser Diode in combination with a photoreceptor was used to measure the global oscillation frequency. The intensity of the reflected beam signal was treated by a Fast Fourier Transform. In these measurements, the laser was placed at an angle with respect to the injection plane vector.
– *LDV (Laser Doppler Velocimetry)*: This device was used to determine the airflow boundary layer profile, at the injectors' lip outlet. To obtain these velocity profiles, the airflow was seeded with magnesium oxide.

3. Qualitative studies

The high speed video camera was an effective tool to visualize the temporal evolutions of the various physical processes during the primary atomization. At this level of detail, it was possible to make a clear distinction between the diverse liquid deformations and the atomization mechanisms. The former term includes the various shapes observed, when a liquid is submitted to aerodynamic forces. A few examples of these structures include the formation of a liquid flat surface (membrane), a thin cylinder (ligament), a low circularity sphere (bulgy droplet).... The latter expression, atomization mechanisms, Fig. 3, refers to a combination of liquid deformations originated by a set of hydrodynamic instabilities, which disintegrate the continuous liquid flow into droplets.

It has been found that a given atomization mechanism influence may be predicted by the momentum flux-ratio:

$$M = \frac{\rho_g v_g^2}{\rho_l v_l^2} \tag{1}$$

where the suffixes (g) and (l) refer to the air and liquid flows respectively. Optionally, multiplying this number by a ratio of characteristic lengths (t_g/t_l), the Air-to-Liquid momentum ratio can be obtained. In this research, (t_g), (t_l) were the air duct edge and the liquid sheet thickness and their ratio equalled 153.

For the values of M, corresponding atmospheric conditions testing, two atomization mechanisms were observed: the Cellular Break-up, Fig. 3a and the Stretched Ligament Break-up, Fig. 3b. The reasoning behind these names lies in the characteristic liquid deformations, observed for the first time by Stapper and Samuelsen [12]. On the other hand, in the model proposed by Mansour and Chigier, these regimes were referred as dilational and sinusoidal modes due

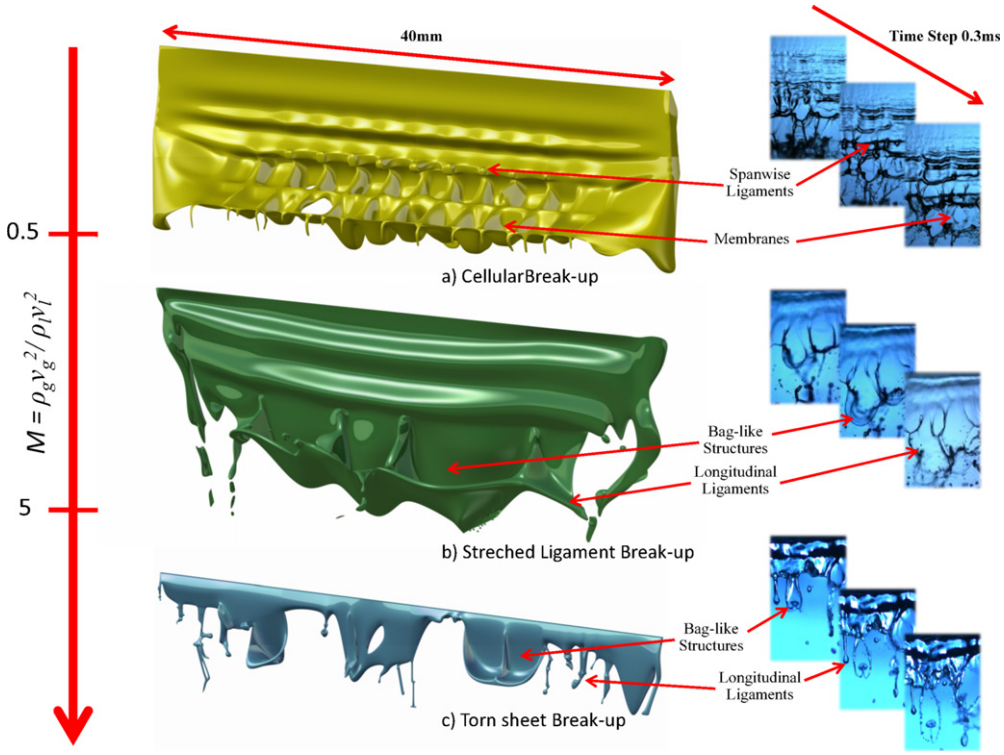

Fig. 3. Atomization mechanisms evolution with momentum flux ratio.

to the waves found on the liquid film. It should be commented though, that in the presented experimental threshold, no varicose waves were observed.

It was found that for values of M below 0.50 the Cellular break-up regime was predominant, while above this limit, the stretched ligament break-up was visible. This border value, has already been proposed by Lozano et al., for one of their atomizers [13]. Both atomization mechanisms showed the same droplet generation means, even if their corresponding influence was different:

– *Membrane Puncturing*: In the first regime, Fig. 3a, it may be seen how membranes or "cellules" were formed between the ligaments. In the second, Fig. 3b, "bag-like" structures were formed instead. These shapes remind to the bag break-up in the secondary atomization phenomena [14]. The droplets produced were of the order of the 50 μm, and hence, could not be accurately quantified with the current experimental set-up. Nevertheless, it may be declared that this droplet generation method contribution was negligible in the cellular break-up regime.
– *Ligament Disintegration*: In the figure above, it might be noticed how spanwise and streamwise ligaments were formed. For the Cellular Break-up, the spanwise ligaments were predominant with droplets, whose diameters reached values greater than the liquid sheet thickness. In the Stretched ligament break-up, the longitudinal structures were similar in diameter, always below the liquid sheet thickness, but with a greater length, of the order of the longitudinal wavelength.

The airflow momentum influence on a liquid sheet has been accounted in previous studies [8,12]. The conclusion was that, as long as the fluid velocities were constant, an alteration in the airflow momentum would not affect the atomization mechanisms basic behaviour. In this research, however, the variation in air momentum was accomplished by adapting the airblast atomizers' dimensions. In the current analysis, keeping the geometry constant, it was possible to modify the airflow momentum, by changing the airflow velocity and/or the airflow density. From the visualizations, it was observed that as long as, the air–water momentum flux ratio remains constant, the atomization mechanism influence is the same. Nonetheless, the liquid deformations would be affected, as it will be showed in the following quantitative section.

Finally, as the magnitude of the M increased above a value of 5, a new atomization mechanism was seen, Fig. 3c. To the authors' best knowledge, no detailed description about this atomization mechanism had been attempted before. Unlike the previous atomization mechanisms, neither spatial nor temporal pattern could be found in the water disintegration. In this article, the atomization mechanism will be referred as Torn Sheet Break-up, due to the shear effect, on the liquid sheet. According to the visualizations performed, it was possible to distinguish the three droplet generation modes:

- *Streamwise ligament disintegration*: This regime was characterized, by the formation of highly irregular shaped, longitudinal ligaments. These were longer and thicker than their counterparts at lower momentum flux ratios. The disintegration of these structures was not strictly ruled by the Rayleigh instability, as the majority were torn away, before the instability could propagate.
- *Membrane puncturing*: As it may be seen, in the previous figure, the formation of bag-like structures did not only occurred in the continuous liquid zone but in the very streamwise ligaments, as well. A similar behaviour was observed in [15], for single liquid jets submitted to relatively high aerodynamic forces. This is known liquid jet membrane-type break-up.
- *Sheet disintegration*: at the highest values of M, the continuous liquid region was eventually torn away in the form of big bulgy droplets. As no spanwise ligaments were formed, the perforations in the continuous region propagated inevitably wind down, fragmenting the liquid sheet.

As for the previous regimes, this atomization mechanism influence was not a function of the airflow momentum but of M. Once the experiments at high pressure were concluded, the tests were repeated at ambient conditions, with a liquid injection velocity of 0.5 m/s. The torn sheet break-up remained dominant.

4. Quantitative studies

The previous references, lead towards remarkable insights of the primary atomization behaviour, at ambient conditions. Nonetheless, additional studies are needed at high pressure environments [16–18]. In this article, we included the results corresponding to the global oscillation frequency, the break-up length and the transversal wavelength. It should be emphasized that in these measurements, the airflow velocity was kept constant, as the absolute pressure increased.

4.1. Global oscillation frequency

As mentioned before, the longitudinal instability in the liquid sheet has been justified by a Kelvin–Helmholtz instability type [11]. A two parallel fluid flows, whose densities and velocities are different, become unstable once they suffer a perturbation. The surface tension forces would damp this perturbation, and hence, deform back the protuberance. However, at this point, the airflow experiences a local static pressure rise, as the local velocity decreases close to the protuberance. Therefore, the aerodynamic forces act as an unstable mechanism. The variable named global oscillation frequency corresponds to the wave generated by this fluids' instability. Its interest lies on its influence on the droplet generation rate.

In Fig. 4, the global oscillation frequency magnitude has been plotted versus the air velocity for a sample of the tested conditions. As expected, there was a linear relation between the oscillation frequency and the air velocity. From the graph, it may be appreciated how the liquid velocity had a weaker effect on the oscillation frequency. Nevertheless, for a 2 m/s injection velocity, the liquid sheet saturated at higher frequencies. As it may be observed from the graph, an increment of the absolute airflow pressure translated into a frequency rise. It is concluded that as the energy per unit volume of air increased, so did the energy transferred to the liquid. In the case of a 1 m/s liquid injection velocity, the saturation occurred between 300 and 400 Hz. This saturation region remained constant as the air pressured increased. It should be noticed, how the global oscillation frequency showed the same behaviour for each atomization mechanism. The exception lied, though, at the highest values of the momentum flux ratio, in the Torn Sheet break-up. The noise generated by additional liquid instabilities hindered the observation of any dominant frequency, using the current technique.

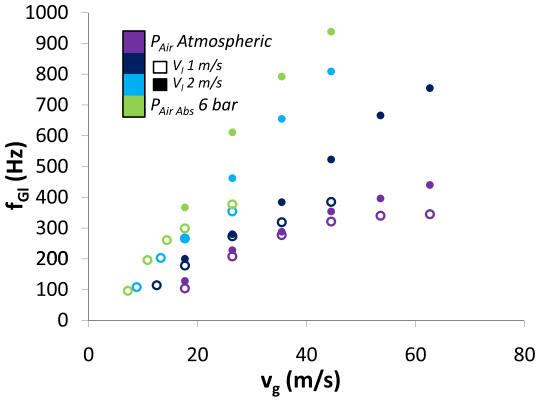

Fig. 4. Global oscillation frequency versus air velocity.

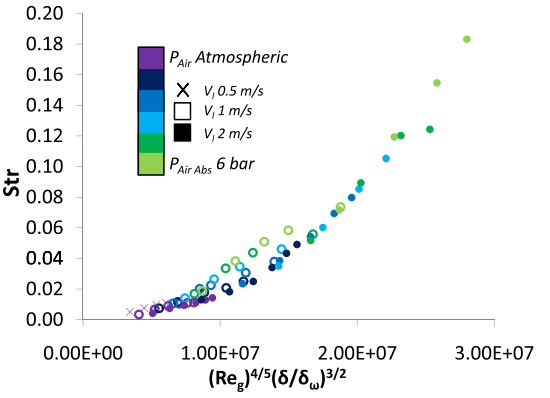

Fig. 5. Global oscillation frequency dimensionless format.

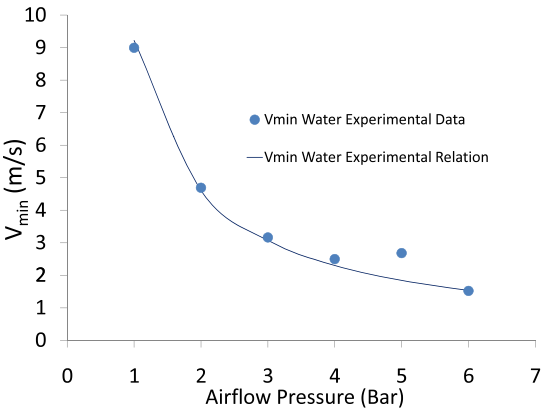

Fig. 6. Minimum oscillation air velocity versus absolute pressure.

As it was showed by Lozano et al. [13], there was a minimum air velocity, at which the longitudinal oscillation was initiated. In these experiences, we found the same value measured by Lozano, around the 9 m/s, for water at atmospheric conditions. This parameter has been found to vary with the liquid physical properties (with values below 3 m/s for ethanol and kerosene) but to remain independent of the liquid velocity. To obtain this parameter, at each pressure value, a trendline was plotted for the points before the liquid sheet saturation. To increase the accuracy of the interpolation at the high pressure environments, the air velocity was reduced up to 6.5 m/s (the lowest airflow velocity possible in the presented set-up). The value, at which these trendlines cut the horizontal axis, marked the magnitude of the minimum oscillation air velocity. In Fig. 6, its magnitude was plotted versus the absolute pressure. The following equation (2), supported by the experimental results, was found convenient to predict the value of the minimum air velocity. The trendline from this equation has also been plotted in Fig. 6:

$$V_{min} = 2 \times 10^{-4} \frac{\sigma_g}{\mu_l} \frac{\rho_l}{\rho_g} \tag{2}$$

This minimum air velocity was proportional to the fluids surface tension, which damped the oscillation and inversely proportional to the dynamic viscosity, which enhanced the energy transfer. From this results it is concluded that the viscosity plays an important effect at low airflow velocities, unlike in the Kelvin–Helmholtz instability definition. This equation has been validated with kerosene. Future research will be directed towards further insight into this instability origin.

Following the example of Larricq, we attempted a dimensional analysis on the results. The description of oscillating flow mechanisms, in a dimensionless format, is commonly done through the Strouhal number:

$$Str = \frac{f_{Gl} t_l}{V_{min}} \tag{3}$$

where t_l is the liquid sheet thickness. In order to express the frequency behaviour, in addition of the minimum oscillation velocity, knowledge of the boundary layer is essential. An analysis of the Kelvin–Helmholtz instability, such as the one in [19], showed that its growth rate was proportional to $\Delta V/\delta_\omega$, where ΔV is the fluids relative velocity and δ_ω is the vorticity thickness:

$$\delta_\omega = \frac{v_g - v_l}{(\frac{\mathrm{d}v_g}{\mathrm{d}y})_{wall}} \tag{4}$$

Following this theoretical analysis, it was sensible to assume the global oscillation frequency to be a function of the instability growth rate. Furthermore, in this model, the vorticity thickness has been assumed independent of the streamwise coordinate, except for values considerably greater than longitudinal wavelength. This assumption agreed with the measurements performed. In Fig. 5, the dimensionless form of the global oscillation frequency was expressed as the product of the Reynolds number times the boundary layer by the vorticity thickness ratio:

$$\frac{f_{Gl} t_l}{V_{min}} = \left(\frac{\rho_g (v_g - V_{min}) c_{Inj}}{\mu_l}\right)^{\frac{4}{5}} \left(\frac{\delta}{\delta_\omega}\right)^{\frac{3}{2}} \tag{5}$$

Under this formulation, convergence was obtained for all the data points. This equation provided a better fit for the measurements at high pressure, than that derived by Lozano, in which the flows' Strouhal number was a function of the air to liquid momentum ratio. Nevertheless, it would be appropriate to change the Strouhal number characteristic length, by the square root of the product of the air and liquid characteristic lengths. As in their tests the liquid and airflow thickness gaps influence was considered, unlike in the current research.

4.2. Break-up length

The break-up length has been defined as the distance from the injector's edge to the end of the continuous liquid region. This variable has a considerable influence in the final spray penetration. In the case of the stretched ligament break-up and the cellular break-up, this length could be unambiguously measured. Conversely, this was not the case in the torn sheet break-up. In this research, the break-up length was defined as the distance from the injector's lips to the longitudinal ligament formation. In Fig. 7, the break-up length was plotted versus the air velocity for a 1 m/s liquid velocity, for each tested pressure and with the extra measurement at 0.5 m/s. It may be gleaned how this length was proportional to the liquid dynamic pressure and inversely proportional to the airflow value. The previous definition of continuous liquid region proved to give homogeneity in the results at all atomization mechanisms. These measurements were consistent with those from oscillometry. As the liquid sheet was energized at a greater rate, it broke-up closer to the injector. The study performed by Larricq established that the break-up length divided by the liquid sheet thickness was a function of the momentum flux ratio times the Weber number, whose characteristic wavelength was the boundary layer thickness. The first dimensionless number accounted for the influence of the atomization mechanism. The second stated the fact that the break-up length is proportional to the surface tension forces and inversely proportional to the airflow inertia. Once this equation was applied, convergence was not obtained at high pressure. Researchers such as Carvahlo [7], have included in their relation the Re_l in order to account for the liquid turbulence. In the current analysis, the liquid to air velocity ratio had a stronger effect on the break-up length:

$$\frac{L_b}{t_l} = \left(\frac{\frac{v_l}{v_g}}{MWe_{t_l}}\right)^{\frac{1}{3}} \tag{6}$$

The graph plotted in Fig. 8, showed the data measured at all tested conditions. It may be argue that there was not complete convergence. The points not fitting the line corresponded to the lowest relative velocities. At these conditions the liquid edges of a planar geometry still formed an angle (check the detail in Fig. 8). This injection geometry was more stable, and hence, it delayed the liquid sheet atomization to greater break-up lengths.

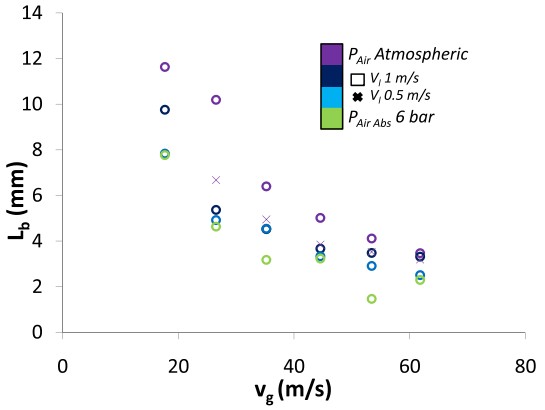

Fig. 7. Break-up length versus air velocity.

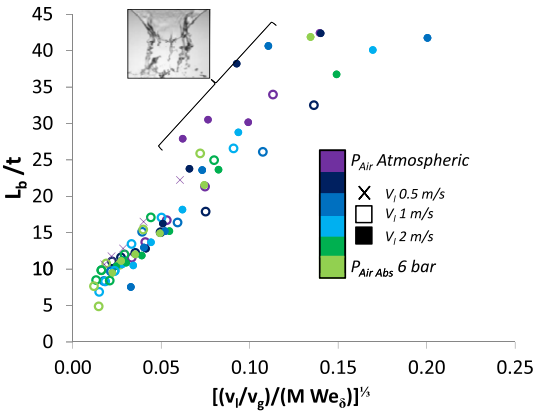

Fig. 8. Break-up length dimensionless format. Detail: sheet geometry at low relative velocity.

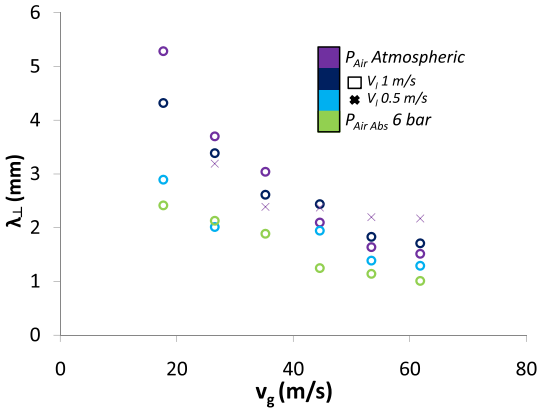

Fig. 9. Transversal wavelength versus air velocity.

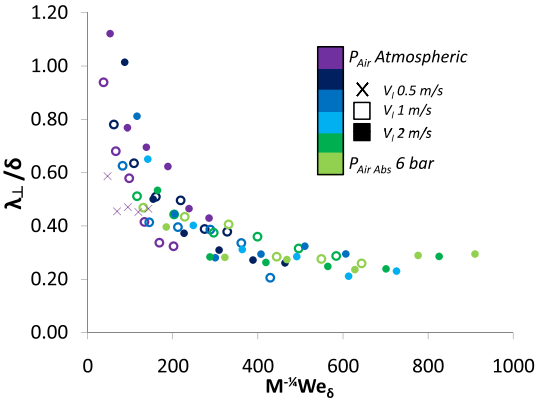

Fig. 10. Transversal wavelength dimensionless format.

4.3. Transversal wavelength

In determining the droplet generation rate, the transversal separation between ligaments is an important factor: It gives an estimation of the longitudinal ligaments number, and hence, the rate of droplets generated by this liquid deformation. Furthermore, Marmottant and Villermaux [20] showed the strong relation between this length scale and the droplets diameter.

No consensus on the transversal oscillation origin has been reached. On the one hand, for the cellular break-up, where non-longitudinal ligaments are formed; this wave might be justified by the Rayleigh–Plateau instability. The crests and troughs in the liquid sheet may be approximated to falling cylinders, through which the oscillation propagates. The same behavior may be observed in the research developed by Davy and Loustalan [21], in an annular liquid sheet. In this publication, it may be observed how in airflow absence, but in an air high pressure environment, the cellular break-up arose. Furthermore, this instability behavior would explain why the droplets generated from these ligaments reached a value above the liquid sheet thickness. On the other hand, even if has been globally accepted that the longitudinal ligaments are a result of the airflow, it is not clear how this phenomenon occurs. As the Kelvin–Helmholtz plays an important effect in the atomization mechanisms, it has been declared to be related to this instability [22].

In Fig. 9, the transversal wavelength has been plotted versus the airflow speed for all tested conditions. An initial observation confirmed the principles of the Rayleigh instability, by which, this wavelength was inversely proportional to the airflow velocity. Nevertheless, a more careful observation revealed a lack in homogeneity. The consequence of plotting results from different atomization mechanisms. As the momentum flux ratio increased, getting further into

the torn-sheet regime, consecutive ligaments could not always be captured, in this time basis measurement. These "missing ligaments" affected the magnitude of the final averaged value. At all tested flow conditions, the smaller wavelength, which could be determined was 1 mm. Taking as hypothesis that the transversal wavelength depends on the atomization mechanism, to be proportional to the inertial forces and inversely proportional to the surface tension forces; the dimensional analysis resulted in:

$$\frac{\lambda_{\perp}}{\delta} = M^{-\frac{1}{4}} We_{\delta} \tag{7}$$

A careful examination of the graph in Fig. 10, showed that for a water velocity of 2 m/s, this relation provided a good convergence for all absolute pressure values. However, at an injection velocity of 1 m/s, where torn sheet break-up had a greater influence, the transversal wavelength started to increase due to this lack of consecutive ligaments.

5. Conclusions

A modest increased in the airflow absolute pressure provided a valuable insight into the primary atomization phenomena. It was confirmed that the momentum flux ratio may be used to predict the appearance of the diverse atomization mechanisms. A new atomization mechanism: the torn-sheet break-up has been characterised. Furthermore, as predicted by M, this atomization mechanism was also observed at atmospheric conditions at very low liquid injection velocities. Future research will include the results obtained at higher pressure values for both water and kerosene. The final objective is using these experimental relations for the liquid sheet physical quantities to predict the droplet size generated.

For the variables, hereby presented, it may be concluded:

- The global oscillation frequency had its magnitude increased with the raise in absolute pressure. Still, it showed the same behaviour at all pressure conditions as well as every atomization mechanism. The exception, however, lied in the highest value of M where the signal noise hindered the measurements. The minimum air velocity, at which this oscillation started, was found to be predicted by the fluids physical properties.
- The break-up length was established as the length from the injector exit to the formation of longitudinal ligaments. Under this assumption the variable showed the same behaviour at all pressure values. As expected, its value was inversely proportional to the air pressure.
- A time basis measurement on the separation between ligaments was accomplished. The dimensional analysis showed a certain degree of convergence in the results. However, the measuring procedure tended to overestimate the measurements in the torn-sheet regime. This was due to the fact that consecutive ligaments did not formed uniformly in time. Overall, the transversal wavelength decreased with the back pressure.

Acknowledgements

This research project has been supported by a Marie Curie Early Stage Research Training Fellowship of the European Community's Sixth Framework Program under contract number MEST-CT-2005-020426.

References

[1] F. Savart, Mémoire sur le choc de deux veines liquids animées de mouvement directement opposés, Ann. De Chim. 55 (1833) 257–310.
[2] C. Larricq, Etude de la pulverisation assistée en air d'une nappe liquid et influence d'un vent ionique sur les intabilités hydrodinamiques, Ph.D. thesis, ONERA, Toulouse, 2006.
[3] F. Couderc, Développement d'un code de calcul pour la simulation d'écoulements de fluides non miscibles. Application à la désintégration assistée d'un jet liquide par un courant gazeux, Ph.D. thesis, ONERA, Toulouse, 2007.
[4] A.H. Lefebvre, Atomization and sprays lecture notes, in: N. Chigier (Ed.), Combustion an International Series, vol. 11, 1989, p. 7.
[5] P. Berthoumieu, H. Carentz, A. Muller, Video techniques applied to the characterisation of liquid sheet break-up, in: 9th International Symposium on Flow Visualization, 2000.
[6] N. Chigier, C. Dumouchel, Atomization of liquid sheets, in: Prog. Astronaut. Aeronaut., vol. 166, 1996, pp. 241–259.
[7] I.S. Carvalho, M.V. Heitor, D. Santos, Liquid film disintegration mechanisms, in: Third International Conference on Multiphase Flow, ICMFi98, Lyon, France, 1998.
[8] A. Lozano, F. Barreras, C. Siegler, D. Löw, The effects of sheet thickness on the oscillation of an air-blasted liquid sheet, Exp. Fluids 39 (2004) 127–139.

[9] B.E. Stapper, W.A. Sowa, G.S. Samuelsen, An experimental study of the effects of liquid properties on the break-up of a two-dimensional liquid sheet, in: Gas Turbine and Aeroengine Congress and Exposition, 1990.
[10] H. Carentz, Étude de la pulvérisation d'une nappe liquide mince, Thèse Université Pierre et Marie Curie, 2000.
[11] A. Mansour, N. Chigier, Dynamic behaviour of liquid sheets, Phys. Fluids A 3 (12) (1991).
[12] B.E. Stapper, G.S. Samuelsen, An experimental study of the break-up of a two-dimensional liquid sheet in the presence of co-flow air shear, AIAA paper 90-0461, 1990.
[13] A. Lozano, F. Barreras, G. Hauke, C. Dopazo, Longitudinal instabilities in an air-blasted liquid sheet, J. Fluid Mech. 437 (2001) 143–173.
[14] L.-P. Hsiang, G.M. Faeth, Drop deformation due to shock wave and steady disturbances, Int. J. Multiphase Flow 21 (4) (1995) 545–560.
[15] P.H. Marmottant, E. Villermaux, On spray formation, J. Fluid Mech. 498 (2004) 73–111.
[16] K. Matsuura, K. Suzuki, Y. Kurosawa, Effects of ambient pressure on sprays characteristics a high shear type aero-engine airblast fuel injector, ILASS Europe, Japan, 2008.
[17] U. Bhayaraju, C. Hassa, Surface wave propagation and breakup in planar liquid sheets of prefilming airblast atomizers, in: ICLASS Europe, 2006.
[18] F.Z. Batarseh, I.V. Roisman, C. Tropea, Effect of primary spray characteristics on the spray generated by an airblast atomizer under high-pressure conditions, in: ILASS Americas, 2008.
[19] F. Charru, Instabilité non visqueuse des écoulements parallèles, in: Instabilités Hydrodynamiques, EDP Sciences/CNRS Editions, France, 2007.
[20] P. Marmottant, E. Villermaux, Fragmentation of stretched liquid ligaments, J. Phys. Fluids 16 (8) (2004) 2732–2741.
[21] M.H. Davy, P.W. Loustalan, On the sheet breakup of direct-injection gasoline pressure-swirl atomizer, J. Atomization Sprays 17 (2007) 501–528.
[22] C. Dumouchel, On the experimental investigation on primary atomization of liquid streams, J. Exp. Fluids 45 (2008) 371–422.